

---

# EXPERIMENTAL INVESTIGATION ON INTERSTAGE THERMAL ENVIRONMENT OF LAUNCH VEHICLE WITH MULTIJETS IN WIND TUNNEL

---

**J. Lin<sup>1</sup>, C. Cao<sup>1</sup>, Y. Wu<sup>2</sup>, and S. Zhang<sup>1</sup>**

<sup>1</sup>Hypervelocity Aerodynamics Institute of China  
Aerodynamics Research and Development Center  
Mianyang 621000, P. R. China

<sup>2</sup>Beijing Astronautics Systems Engineering Institute  
Beijing 100076, P. R. China

During the stage separation course of a launch vehicle, the environment of the stage is quite serious because of the high temperature and pressure. It is very important to investigate the pressure and heat flux distribution under the interstage thermal environment, as is good for the design of stage configuration. This paper presents the test technique of a thermal environment simulation with multi-jets of the launch vehicle stage separation in 1-meter-diameter hypersonic wind tunnel (HWT). The internal and external flows run simultaneously. A hot jet technique that makes use of five engine jets at the same time is adopted to simulate the internal flow. Pressure and heat flux measurements have also been developed. Pressure, temperature and heat flux characteristics of the first-stage fore-envelop head and the second-stage aft-envelop head which vary with different separation distances and different exhaust windows are introduced. The results indicate that the environment of a small stage separation distance is severe. The smaller separation distance is, the less is the uniformity of pressure, temperature, and heat flux distributions. A coaxial thermocouple is available to measure the heat flux between stages, whereas the accuracy of the heat flux measurement as well as the heat flux simulation rules need further exploring and studying.

## 1 INTRODUCTION

During the stage separation course of a launch vehicle, high temperature and high pressure jet flow produced by the main working engine of the second stage will

cause a severe influence on the stage environment [1–3]. A wind tunnel presents a test reference for indicating the interstage thermal environment conditions and it is beneficial to optimize the stage configuration. It is very important to investigate the pressure and heat flux distribution under the interstage thermal environment with multijets interaction, as it can improve the thermal protection design.

The paper presents the test technique of a thermal environment simulation with multijets interaction of the launch vehicle stage separation in 1-meter-diameter HWT. The internal and external flows are run simultaneously. The internal flow simulation adopts a hot jet technique which makes use of one main engine and four vernier engines at the same time. Some measurements have also been developed to obtain pressure, temperature, and heat flux distribution characteristics of the first stage fore-envelop head and the second stage aft-envelop head with different stage distance and different exhaust windows.

## 2 TEST SIMULATION METHODS

### 2.1 Test Facility

One-meter-diameter HWT is an intermittent, blowdown hypersonic wind tunnel. It has been equipped with nozzles from Mach 3 to 8, and it can simulate the flight altitude from 20 to 60 km. The tunnel is run with a compressed air store (160 m<sup>3</sup>, at the pressure of 22 MPa), which exhausts into vacuum spheres (4000 m<sup>3</sup>). A storage heater, 2 m in diameter and 12 m in height, can be raised to the maximum temperature of about 760 K by electric heating.

At present, measurement and control systems of the tunnel mainly contain 96-channel data acquisition system, 500-millimeter-diameter Schlieren system, four Degree of Freedom attack angle machine system, DTC Initium electronic scanner pressure measurement system, and other auxiliary systems.

### 2.2 External Flow Simulation

**Table 1** External flow conditions

$M_\infty$	$H$ , km	$P_0$ , kPa	$Re_1$ , 1/m
6	50	120	$1.7 \cdot 10^6$

The external flow of a launch vehicle in a flight is simulated by the flow field in 1-meter-diameter HWT. The main simulation parameters are the freestream Mach number  $M_\infty$  and the flight altitude  $H$  [4], which are presented in Ta-

ble 1 where  $P_0$  is the stagnation pressure of the wind tunnel stilling chamber and  $Re_1$  is the unit Reynolds number.

### 2.3 Internal Flow Simulation

Utilizing the exhaust gas generated by a micro solid rocket engine as a jet medium, a hot jet technique is required to accomplish the correct interstage thermal environment simulation with multijets. By developing two independent micro solid rocket engines, one main engine and four vernier engines around are exhausted simultaneously.

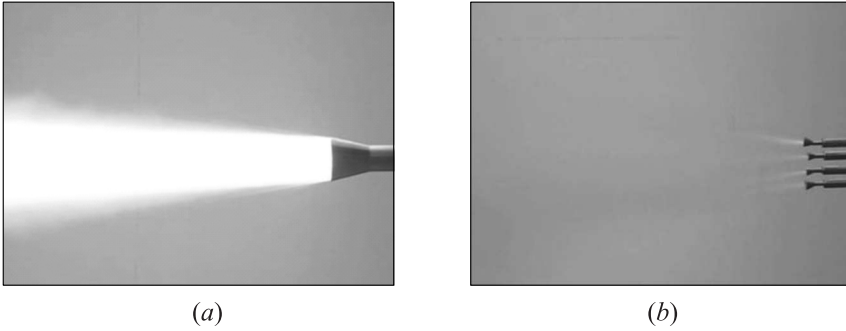


**Figure 1** Testing of main engine (a) and vernier engine (b) ignition in atmosphere environment

With the research work being focused on the interstage thermal environment, the task of simulating a real flight in a wind tunnel becomes really important. The combustion chamber pressure and temperature are ensured on the basis of exhaust nozzle geometric analogy when the solid powder mode of a rocket engine exhaust is substituted for a liquid mode. Furthermore, the ratio of specific heats and the production of the exhaust gas are made close to the real ones by adjusting propellant components. Mach number  $M_j$ , the pressure ratio  $P_j/P_\infty$ , and the temperature of jet are thus able to be simulated analogously. Figure 1 presents the photograph of main engine and vernier engine testing, respectively, in the atmosphere. Internal flow conditions are listed in Table 2 where  $T_{0j}$  means the total temperature of jet.

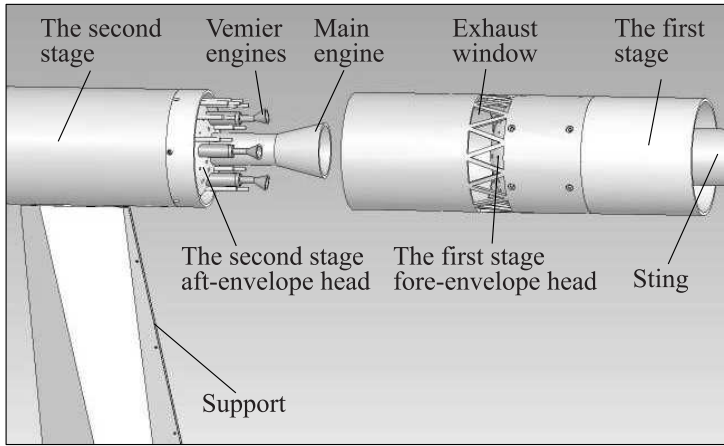
**Table 2** Internal flow conditions

Type	$M_j$	$P_j/P_\infty$	$T_{0j}$ , K
Main engine	3.95	312	3367
Vernier engine	4.53	63	3046

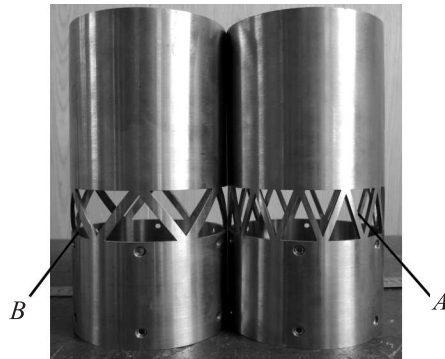
## 3 MODEL DESCRIPTION AND TESTING METHODS

### 3.1 Model Description

As shown in Fig. 2a, the test model is composed of several parts including a first-stage body, a second-stage body, an aft-envelope head, a fore-envelope head,



(a)



(b)

**Figure 2** Test model: (a) model components; and (b) exhaust windows

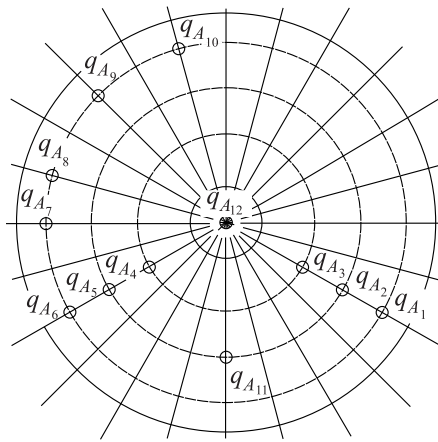
exhaust windows, the main engine and vernier engines, etc. The second stage is mounted to the support facilities with the body's partial lower surface, and the first stage is fixed with a sting system.

In order to study how the exhaust windows influence the interstage thermal environment, two kinds of exhaust windows with different orifices (Fig. 2b), on the condition that the area sum of exhaust window orifices keeps being invariant, are designed. The number of exhaust windows *A* is twice that of orifices as exhaust windows *B*.

The coaxial angle of attack of the two stages is 0 degree, and the ratio of the separation distance to the diameter of the first stage  $X/D$  is 0, 0.1, 0.3, 0.5, and 1.0, respectively.

### 3.2 Testing Description

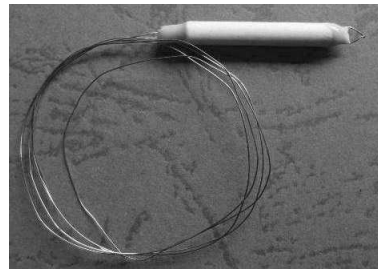
There are several measurement points disposed orderly on the surface of the first-stage fore-envelope head in order to study interstage thermal environment during the separation, including twelve pressure points  $P_{A_i}$ , twelve temperature points  $T_{A_i}$ , and twelve heat flux  $q_{A_i}$  (subscript  $i = 1 \sim n$  denotes the sequence of measurement points). The center point is  $q_{A_{12}}$  with  $P_{A_{12}}$  upward and  $T_{A_{12}}$  downward. The second-stage aft-envelope head surface has been disposed ten pressure points  $P_{B_i}$ , ten temperature points  $T_{B_i}$ , and ten heat flux  $q_{B_i}$ , which are one-to-one corresponding to those of the first stage. The heat flux point distribution on the first-stage fore-envelope head is shown in Fig. 3a as an example, it is the same as the pressure and temperature point distributions are.



(a)



(b)



(c)

**Figure 3** Measurement point disposition and sensors: (a) heat flux measurement points; (b) coaxial thermocouple; and (c) WRe3-WRe25 thermocouple

The environment of the stage is serious owing to the high temperature and high pressure; so, it is very important to choose the right testing element. A coaxial thermocouple, whose diameter is 3 mm, is employed as a sensor to measure the heat flux of the envelope head surface (Fig. 3*b*). Its measurement scope is from  $100 \text{ kW/m}^2$  to  $20 \text{ MW/m}^2$  and the precision is less than 20%. To measure the surface temperature, a thermocouple made up by WRe3-WRe25 is used whose measurement scope is from 0 to  $2500 \text{ }^\circ\text{C}$  and the precision is less than 1% (Fig. 3*c*). The envelope head surface pressures of two stages are measured by the pressure transducer, and its precision is less than 0.3%.

## 4 RESULTS AND ANALYSIS

### 4.1 Flow Structures

The typical Schlieren photos of the hot jet flow field with the different stage distances and exhaust windows are shown in Fig. 4. The flow jetting from the second

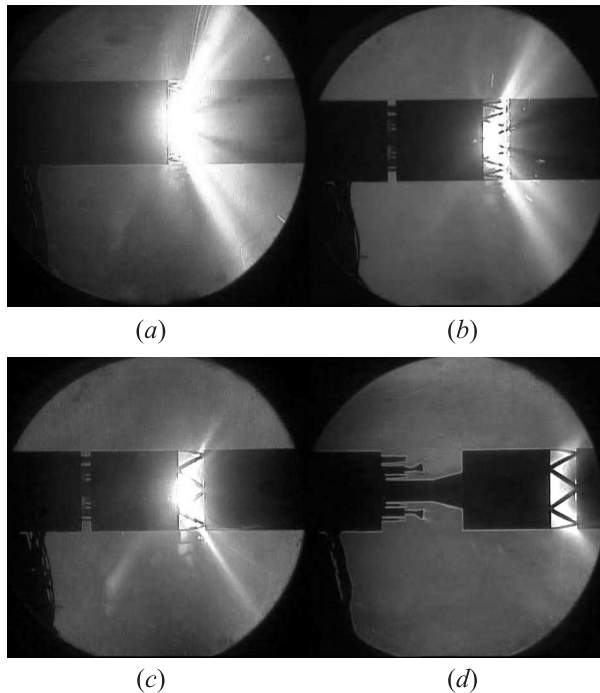


**Figure 4** Schlieren photograph of hot jet flow field with different stage distances and exhaust windows; exhaust windows A: (a)  $X/D = 0$  and (b)  $X/D = 0.1$ ; and exhaust windows B: (c)  $X/D = 0.1$  and (d)  $X/D = 1.0$

stage clashes the fore-envelope head of the first stage and is thoroughly blocked. The majority of the exhaust plume emits from the exhaust window while the remainder reflects back and ejects from the gap of stages. The shock interacts strongly with the complicated viscous flows of the first-stage fore-envelope head, so that a bow shock is very obviously displayed. The strength of the bow shock is weakened with the increment of the stage distance. The flow field near the exhaust window is brightened by the high temperature gas in the amount enough to thereby conceal wave flow details, so there is no clarity in the flow phenomena of the stage gap.

## 4.2 Test Data Analysis

### 4.2.1 Pressure distributions

The dimensionless pressure distribution curves vs. a measurement point with different exhaust windows are shown in Fig. 5a when a stage distance equals zero. Since the first-stage fore-envelope head is subject to the normal jet impact, the pressure values about the center are much higher than those near the border. The values of the pressure on the second-stage aft-envelope head are far lower than on the first-stage fore-envelope head. If the area sum of exhaust window orifices is kept invariant, the increment of each exhaust window orifice's area, that is the quantity of window orifices decreases has a small effect on the pressure of the first-stage fore-envelope head, while a rapid change occurs on the second-stage aft-envelope head where pressure values increase greatly.

Figure 6a displays the pressure variation with different stage distances on the measurement point  $A_7$  near the border of the first-stage fore-envelope head, the point  $A_{12}$  near the center, and  $A_4$  between  $A_7$  and  $A_{12}$ . The pressure values on  $A_{12}$  are higher than  $P_{A_7}$  as the stage distance  $X/D$  is not longer than 0.3. A similar phenomena occur when  $X/D$  is 0.8 up to 1.0. Around the distance of 0.5, there is a trend of the pressure values on  $A_{12}$  to be less than  $P_{A_7}$ .

### 4.2.2 Temperature distributions

The temperature distribution curves vs. a measurement point, with different exhaust windows on different heads, are shown in Fig. 5b when a stage distance equals zero. The points on the first-stage fore-envelope head are at a high level of temperatures (from 2200 to 2600 K) with the highest temperature at the head center. Temperatures on the second-stage aft-envelope head range from 320 to 700 K, that is, they are much lower than those on the first-stage fore-envelope head. The cause is that majority of the exhaust plume emits from the exhaust window, leaving a minority flow which returns to influence the second stage. The temperature curves vary similarly to pressure curves.

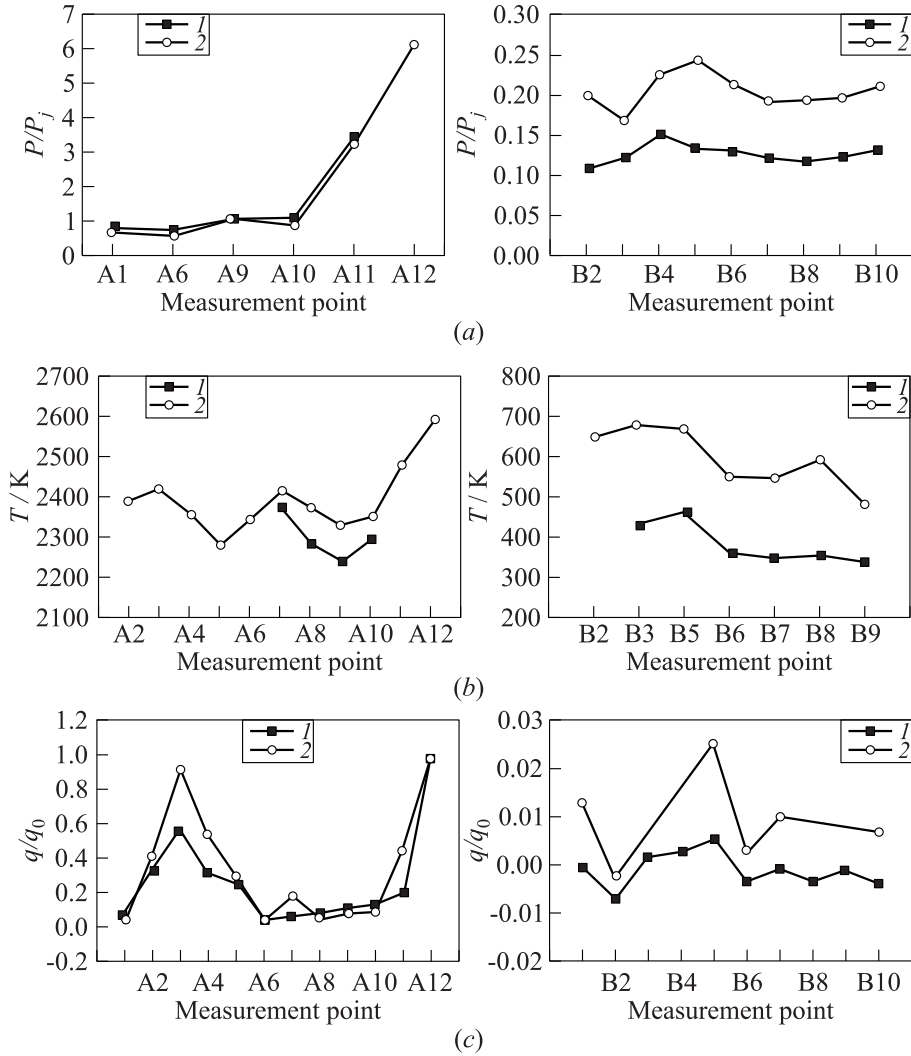


**Figure 5** Pressure (a), temperature (b), and heat flux (c) distributions with different exhaust windows (1 — A and 2 — B) on first-stage fore-envelope head (left column), and on second-stage aft-envelope head (right column) when  $X/D = 0$  vs. measurement points

The temperature variations with different stage distances on measurement points  $A_7$ ,  $A_{12}$ , and  $A_4$  are displayed in Fig. 6b. The temperature value  $T_{A_{12}}$  largely decreases with the increment of the stage distance, as point  $A_{12}$  is very near the center of the first-stage fore-envelope head. Temperature  $T_{A_7}$  is nearly

equal to  $T_{A_{12}}$ , while  $T_{A_4}$  is the highest among the three measurement points when  $X/D$  is not shorter than 0.5.

**4.2.3 Heat flux distributions**

The dimensionless heat flux distribution curves ( $q$  divided by  $q_{A_{12}}$ ) vs. measurement point with different exhaust windows are shown in Fig. 5c. Similarly to pressure and temperature variations, the heat flux values on the first-stage fore-envelope head are much higher than those on the second-stage aft-envelope head. The heat flux difference between two exhaust windows is little on the first-stage fore-envelope head, while on the second-stage aft-envelope head, the heat flux values with exhaust windows  $B$  are higher than with exhaust windows  $A$ .

The heat flux variations with different stage distances on measurement points  $A_7$ ,  $A_{12}$ , and  $A_4$  are displayed in Fig. 6c. The value  $q_{A_{12}}$  largely decreases with the increment of the stage distance.  $q_{A_4}$  increases but decreases at the distance of  $X/D = 0.5$ . When  $X/D$  is not shorter than 0.5,  $q_{A_4}$  is the highest among the three measurement points, and  $q_{A_7}$  is nearly equal to  $q_{A_{12}}$ .

**5 CONCLUDING REMARKS**

The thermal environment between launch vehicle stages and one main engine with four vernier engines around exhausting simultaneously are simulated

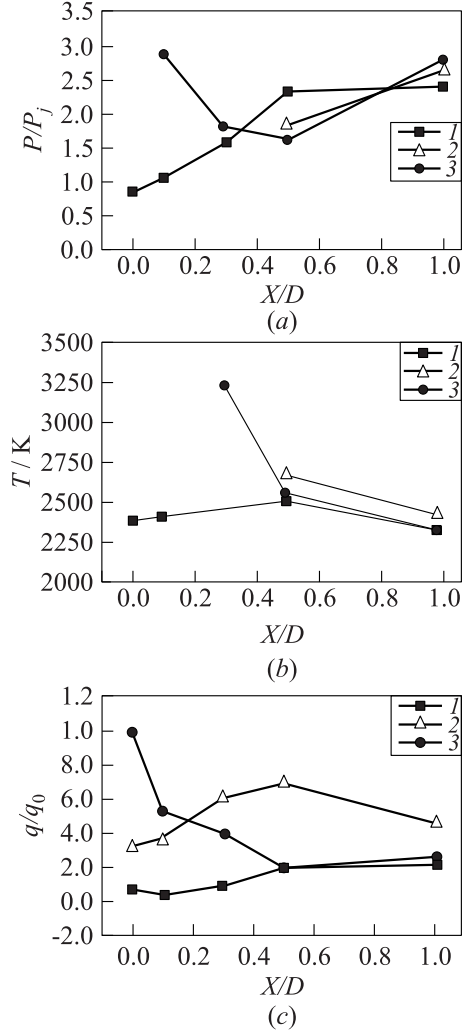


**Figure 6** Pressure (a), temperature (b), and heat flux (c) distributions of different measurement points on first-stage fore-envelope head with exhaust windows A (1 —  $A_7$ ; 2 —  $A_4$ ; and 3 —  $A_{12}$ ) vs.  $X/D$

in  $\phi = 1$  m HWT using a hot jet technique. The heat flux, temperature and pressure distributions are obtained on the surfaces of the first-stage fore-envelope head and the second-stage aft-envelope head. The test results show that the shorter stage distance is the more serious is the separation environment. The first-stage fore-envelope head is impacted directly by jets and, consequently, gives rise to the great variation of the physical distributions. The second-stage aft-envelope head, however, causes far less impact than the first-stage fore-envelope head. The quantity change of the exhaust window orifices has few effects on the heat flux, temperature and pressure distributions of the first-stage fore-envelope head if the area sum of exhaust window orifices is kept invariant, when the separation distance  $X/D$  equals zero. However, this influence on the second-stage aft-envelope head is quite obvious under the same condition. The heat flux, temperature and pressure values of the second-stage aft-envelope head increase as the quantity of the exhaust window orifices decreases. The presented test technique can be taken as a reference method for predicting the thermal environment between launch vehicle stages, and the results indicate the applicability of coaxial thermocouple for measuring the heat flux. Nevertheless, the accuracy of the heat flux measurement and the heat flux simulation rules still need to be further improved and studied.

## ACKNOWLEDGMENTS

This work was partially supported by China National Natural Science Foundation (No.11002155), and the first author would like to thank Dr. Liu Xin of CARDG for his constructive suggestions.

## REFERENCES

1. Wan, Y. 1992. Aerodynamic design of stages and influence of plume flow separation on aerodynamic characteristics of launch vehicle. *J. Astronautics* 2:95–98.
2. Bannink, W. J., E. M. Houtman, and P. G. Bakkker, 1998. Base flow/underexpanded exhaust plume interaction in a supersonic external flow. AIAA Paper No.98-1598.
3. Han, S., and F. Guo. 2002. Research of a new method of stage separation. *J. Astronautics* 23(4):47–51.
4. Yun, Q. 1991. *Experimental aerodynamics*. Beijing: National Defence and Industry Press.